

Effect of Angle on Particle Deposition in an Impingement Jet

T.G. Walmsley¹, M.R.W. Walmsley¹, S. Zhao¹, J.R. Neale¹ and M.J. Atkins¹

¹School of Engineering

University of Waikato, Hamilton, New Zealand

Abstract

Experimental tests and computational fluid dynamics (CFD) models of an impingement air jet have been applied to deposition of sticky particles at two impingement angles, normal and 45°. Models have been verified using Particle Image Velocimetry (PIV) for the air jet flow field and particle-wall contact and deposition. Particular attention has been given to the particle-wall boundary interaction and the effect of tangential versus normal velocity components on predicting deposition.

Results reveal unique deposition morphologies which vary with jet velocity, angle of jet impingement, and stickiness of the particles. Defined rings of deposits have been observed at both impingement angles. Less sticky particles impact the plate, bounce one or more times, before depositing. Deposition from an impingement angle of 45° showed elliptical rings skewed towards the obtuse angled side. The acute angle side of the impingement jet contained a small highly deposited region, with the outer regions having almost no deposition. CFD models under predicted the total deposition percentage. A lower deposition percentage for acute angle impacts, at the same average jet velocity and particle stickiness, confirmed tangential velocity aids in fracturing liquid bridges. The extent tangential velocity aids fracture is strongly dependent on particle size and contact area of the liquid bridge.

Introduction

Air impingement jets are a topic extensively covered in the literature [7]. Numerical modelling of impingement jets has also been a focus of several studies [1,4]. Most investigations are for jets impinging normal to a plate, rather than at an angle. Application of particle deposition in impingement jets are mostly found in the powder spray coating and aerosol literature, which desire an even spread of deposition [3]. More recently impingement jets have been used to better characterise critical sticking conditions of food powders [10]. Results are now being applied to numerical models to predict deposition amounts and patterns, so that deposition can be minimised [12]. Improved deposition control through numerical models have the potential to be applied to ultraclean integrated circuit manufacturing, air pollution control, therapeutic drug delivery in human airways and food powder processing.

Studies using an impingement jet deposition test have shown that deposition tendencies are strongly affected by air flow dynamics and particle size distribution, in addition to stickiness as a result of air temperature, air humidity and the amorphous composition of the particles [14]. With sufficient understanding of all variables affecting deposition, models and capture criterion can be formed to predict deposition occurrence and location. Overtime verified numerical air flow models and accurate capture criteria may be developed and applied to enable smart geometric design of processing equipment to minimise powder deposition.

Factors contributing to deposition of amorphous powder

Experimental studies on deposition of amorphous powder have focused on measuring the critical temperature and relative humidity conditions that result in powders adhering to walls, for a constant air velocity, impingement angle and size distribution. Amorphous composition, temperature (T) and relative humidity are used to define the surface stickiness of particles. Relative humidity and water activity are related to the glass transition temperature (T_g) through a variant of the Gordon-Taylor equation [5] or other polynomial models [2]. The amount the air temperature is above the corresponding T_g value, i.e. $T - T_g$, has been shown to be logarithmically related to viscosity [13] and successfully applied as a measure of stickiness. Viscosity is intricately related to a particle's ability to form liquid bridges. $T - T_g$ for several amorphous food powders is independent of temperature and humidity [6].

In addition to surface stickiness particle kinetics also strongly influences deposition. Larger particles or an increase in particle impact velocity require more sticky particles to deposit [14]. Impact velocity can be broken down into a normal component and tangential component. The normal velocity component has been the subject of several studies, with less attention given to the effect of the tangential component.

Numerical and Experimental Methods

Experimental deposition in an impingement jet

An impingement jet with a round jet horizontally impinging on a target plate has been used to characterise deposition. The impinging air is conditioned to a required temperature (73 to 80 °C) and relative humidity. Sub 100 micron skim milk powder (SMP) is gravity injected into the air flow following a Venturi point. Particles mix with the conditioned air down a calming length of 756 mm, a length to diameter ($D = 11$ mm) ratio of more than 60. After exiting the end of the round tube, the particle laden air impacts a rectangular stainless steel plate (164 × 136 mm), 44 mm away. The resulting height (H) to diameter ratio is 4.

For all tests an average jet velocity of 10.3 ms⁻¹ impinging at a 0° and 45° to the normal have been studied. Deposition percentage is calculated by weighing the powder deposited compared to the powder injected into the flow. No corrections for deposits in the Venturi have been made. $T - T_g$ values are obtained using the jet temperature and relative humidity. T_g is estimated using the third order polynomial model of [2], by assuming relative humidity and water activity are equal. $(T - T_g)_{crit}$ is found by extrapolating back to the x-axis on a deposition % versus $T - T_g$ plot.

Numerical modelling of impingement jet and deposition wall-boundary condition

The CFD package Fluent 12.1.4 and Gambit 2.4 have been used for modelling the impingement jet. In the model, air enters the domain at an average velocity of 10.3 ms^{-1} through the top of a 756 mm long tube before exiting and impinging against a wall boundary 44 mm away, as measured along the tube centreline. The tube has an internal diameter of 11 mm. Specific details of the models and solution methods are the same as [14].

Fluent's Discrete Phase Model is applied to track particles in the flow domain. Inert particles have been injected into the flow post-processing, with a particle density (ρ) of $1540 \text{ kg}\cdot\text{m}^{-3}$. Since the experimental particle to air volume fraction was about 0.01%, one-way coupling between the particle and the air is deemed valid. The size distribution of injected particles resulted from a Rosin-Rammler log model that matched experimental size distribution.

In the impingement jet model, each time a particle impact the wall, a deposition criterion is evaluated determining whether or not a particle deposits or rebounds. The derivation of equation (1) is based on all particles in a jet of a particular temperature and relative humidity having the same surface adhesion energy density, U_{ad} , as a numerical substitute for particle stickiness. U_{ad} has been shown to relate to $T - T_g$. Particles are assumed to be perfect spheres with no plastic deformation occurring at impact. The weakness of the current model is the lack of understanding as to the role of the tangential velocity component in deposition. The complete derivation of the capture criteria is found in [12].

$$U_{ad} \geq \frac{\rho}{3k^2} d \cdot V_{n,i}^2 \quad (1)$$

where k is the ratio of the contact diameter (d_c) to particle diameter (estimated as 0.4), d is the particle diameter, and $V_{n,i}$ is the initial velocity in the normal direction.

Visualisation of impingement jet airflow patterns

In this study, PIV flow visualisation techniques has been successfully applied to characterise the impingement jet air flow patterns at several average jet velocities (8.0, 10.3, 15.2, 19.4, 25.0, and 35.8 ms^{-1}) and two impingement angles of 0° and 45° to the normal. In essence, PIV uses a thin laser light sheet ($< 1 \text{ mm}$) generally orientated parallel to a fine particle seeded gas or liquid flow. Dispersion of the light sheet caused by the seeded particles is captured by a camera that is fixed perpendicular to the sheet. Two images are taken in very quick succession. Images are compared and processed using cross correlation computer algorithms to successfully compute velocity flow fields of the cameras view.

The experimental set-up and method of applying PIV to an impingement jet in this study is the same as [12]. Parafin liquid has been used as the seed material, and was observed to stick to the plate after impact, although enough particles remained in the air flow to capture the velocity flow field in and around the jet. Maximum velocities in the PIV vector flow fields have been verified using a hand-held TSI hotwire unit. Figure 1 shows PIV velocity flow field results for both angles studies. Shape of the impingement jet did not vary significantly for different jet velocities, hence only the normalised velocity magnitude (v/v_{max}) is present because it is representative of all velocities between 8.0 and 35.8 ms^{-1} .

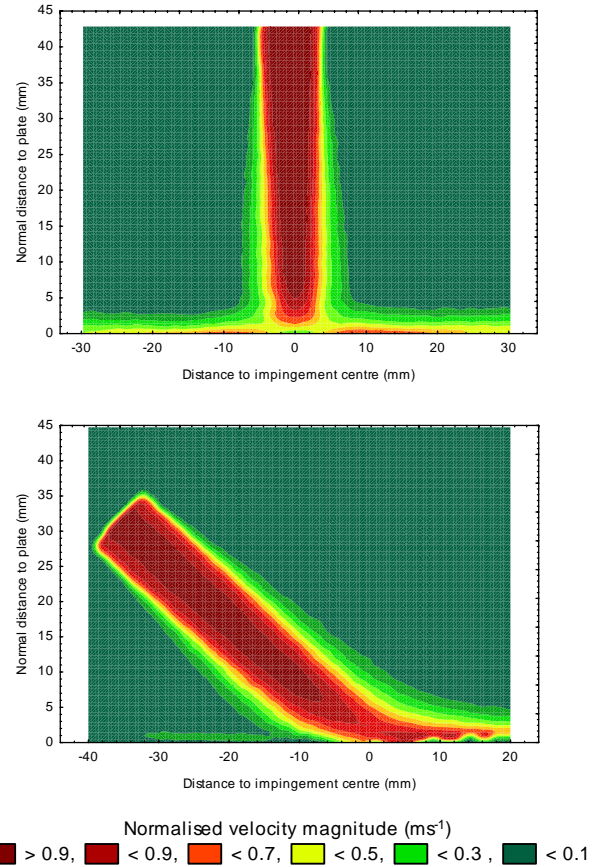


Figure 1. Normalised velocity magnitude contours of an impingement jet with $H/D = 4$, obtained using PIV analysis, at two angles, to the normal: 0° , top and 45° , bottom.

Results

Effect of tangential velocity on $T - T_g$

The effect of increasing tangential velocity is to decrease deposition at the same level of stickiness (figure 2). If the tangential velocity component played no role in affecting deposition, it is expected the deposition trend line to have shifted left of the normal impingement line, and fall on the same line as estimated for a jet velocity 7.3 ms^{-1} at normal impingement, with a $(T - T_g)_{crit}$ of 6.0°C . Hence, the effect of tangential velocity is to increase $(T - T_g)_{crit}$ by 7.4°C .

Results for the effect of tangential velocity are significantly different to other studies. Researchers have assumed the effect of tangential velocity is small compared to the normal velocity [11], and only matters when a critical impact angle is reached causing all particles to rebound [7]. A recent study concluded the angle of impact, for a constant jet velocity and same particle material as this study, had no effect on $(T - T_g)_{crit}$ and reduced the gradient of the deposition trend line, or the rate of deposition [9]. However intuitively, when a particle comes in contact with a wall, it will either stick if the conditions are favourable or rebound. Two significant sources of experimental variation are the width of the particle size distribution and the range of impact velocities occurring at different locations on the deposition plate. This study has obtained a fraction of a normal SMP distribution through the aid of size sieving. The other area of variation results from the size of the deposition plate. This study used a large rectangular plate compared to the 75 mm disc used in [9]. Deposited particles outside the jet impingement zone would have contained a significant tangential velocity component, meaning

the average jet velocity is not representative of all deposited particles. An improvement, therefore, is to use a deposition plate equal in size to the impingement jet diameter.

Reported $(T - T_g)_{crit}$ values are similarly unique to a test set-up, causing some ambiguity in meaning. If measured correctly taking into account particle size, impact velocity and impact angle, $(T - T_g)_{crit}$ has the potential to precisely define particle deposition tendencies. Until this occurs, accuracy and possible unification of $(T - T_g)_{crit}$ literature values for different test methods will be difficult.

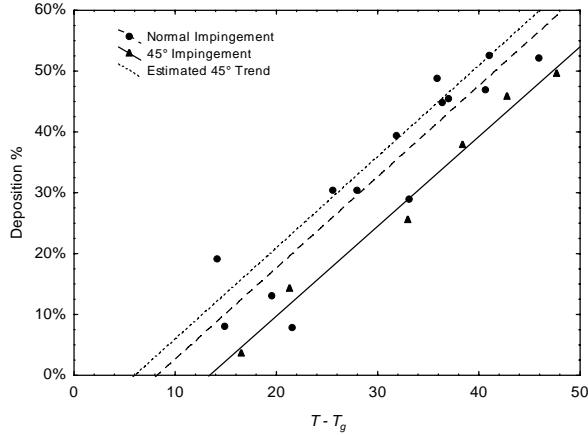


Figure 2. Effect of jet impingement angle on % deposition. $(T - T_g)_{crit}$ is 8.2 °C for normal impingement and 13.4 °C for 45° impingement at 10.3 ms⁻¹, and 6.0 °C for an estimated normal impingement at 7.4 ms⁻¹, the normal component of 45° impingement.

Influence of tangential velocity on particle-wall liquid bridge

Analysis of the liquid bridge bonding a particle to a wall gives a clear mechanistic reasoning for the affect of tangential velocity. Figure 3 shows the resultant forces acting on a particle impacting a wall at an angle. Tangential components of velocity induce a peel action on one side of the liquid bridge acting as a location of stress concentration at point A. F_{tan} is the consequence of a change in particle momentum with time in the tangential direction and is coupled with $F_{friction}$ resulting from particle stickiness forming a liquid bridge. This force couple induces a turning moment, which effectively attempts to lift away the bond on one side. The result is a significant contribution from the tangential velocity to break the liquid bridge.

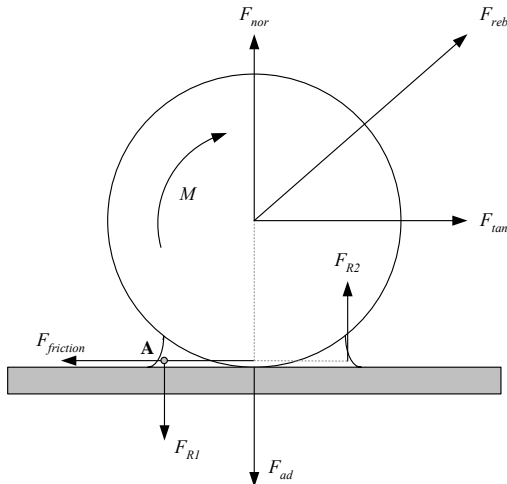


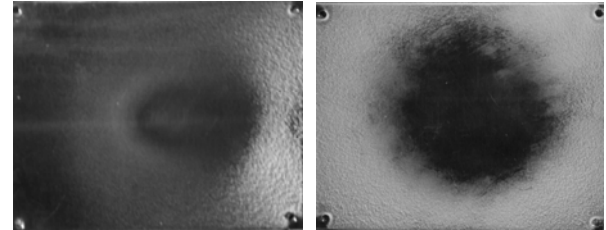
Figure 3. Force (F) and moment (M) balance of a particle at impact.

By applying a force and moment balance, an expression for the maximum stress, σ_{max} , on the adhesion bond is derived. This occurs at point A. Equation 2 contains two terms: the left represents the role of the normal velocity and the right is the tangential velocity contribution. It is thought if σ_{max} at point A exceeds the bond strength, a particle tears away from the surface from one side of the bond (point A) and rebounds at a more acute angle than the impact angle. m is the particle mass.

Experimental and numerical deposition morphologies

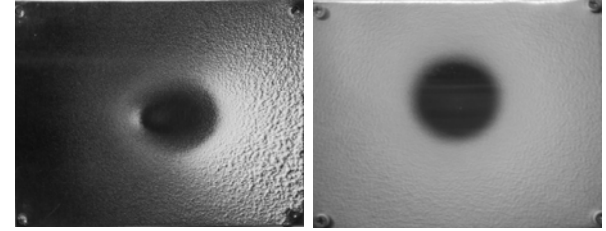
Unique to deposition in an impingement jet is the ring morphology. Rings are produced from particles impacting the wall, bouncing along the face of the wall one or more times before depositing. CFD impingement models have been used with some success to predict deposition and ring shaped patterns for normal impingement jets [12]. Deposition models, however, have rarely been applied to angled impingement jets.

As stickiness of particles is increased, a deposition morphology evolution occurs for both normal and 45° impingement angles (figure 4). At initially low levels of stickiness, few little deposits are found on the plate. As $T - T_g$ is increased, a large ring of the plate appears. Further increase moves the ring closer to the jet centre. At extreme levels of stickiness no centre ring is detected and the majority of particle sticks on first impact. Rings are circular for in a normal impingement and elliptical for 45° impingement. The other significant difference is a small build up of deposits on the acute angle side of the 45° impingement jet (figure 4e). This build up is located at a stagnation point (figure 1). Particles that enter and impact in this zone have slow impact velocities allowing for deposition.



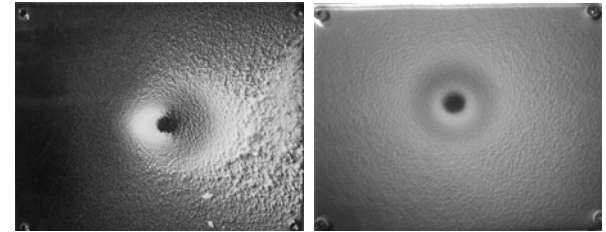
a) $T - T_g$ 16.6 °C and 3.5% Dep.

b) $T - T_g$ = 15.0 °C and 8.0% Dep.



c) $T - T_g$ 24.5 °C and 14.2% Dep.

d) $T - T_g$ 25.7 °C and 30.3% Dep.



e) $T - T_g$ 33.1 °C and 25.5% Dep.

f) $T - T_g$ 35.9 °C and 48.7% Dep.

Figure 4. Evolution of experimental deposit morphologies with increasing $T - T_g$ at air velocity of 10.3 m/s. Left: 45° impingement. Right: normal impingement.

Using the deposition criterion derived by [12], CFD models have been applied to predict deposition in a normal impingement jet and 45° impingement jet (figure 5). Experimental morphologies have been selected to have resulted from similar $T - T_g$ values, and use the same corresponding U_{ad} in CFD predictions [12]. For both angles, the CFD particle deposition % prediction is significantly different to the experimental. This results from the experimental test having a non-uniform temperature and humidity profile along the face of the plate. The clear ring diameter of the normal impingement jet matches well, but the match in the 45° jet is less obvious. The original deposition criterion needs improvement to better account for the effect of tangential velocity.

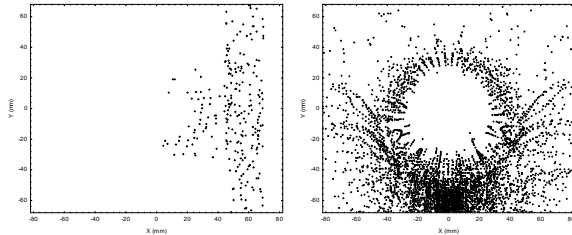


Figure 5. CFD deposit morphology at air velocity of 10.3 m/s and $U_{ad} = 0.001 \text{ J}\cdot\text{m}^{-2}$. Left: % Dep. = 1.3%. Right: % Dep. = 2.7%.

Conclusions

Results show the effect of increasing tangential velocity is to decrease deposition at the same level of stickiness. Numerical analysis also showed the contribution of tangential velocity is significantly affected by particle size, material and impact velocity. Results also reveal unique deposition morphologies which vary with angle of jet impingement and stickiness of the particles. Less sticky particles impact the plate, bounce one or more times, before depositing. Deposition from an impingement angle of 45° showed elliptical rings skewed towards the obtuse angled side. The acute angle side of the impingement jet contained a small highly deposited region due to a stagnation zone, with the outer regions having almost no deposition. A lower deposition percentage for acute angle impacts, at the same average jet velocity and particle stickiness, confirmed tangential velocity weakens the liquid bridge bond.

References

- [1] Angioletti, M., Nino, E. & Ruocco, G., CFD turbulent modelling of jet impingement and its validation by particle image velocimetry and mass transfer measurements. *International Journal of Thermal Sciences*, **44**, 2005, 349-356.
- [2] Brooks, G. F., *The sticking and crystallization of amorphous lactose*. Master of Technology Thesis, Massey University, 2000.
- [3] Burwash, W., Finlay, W. & Matida, E., Deposition of Particles by a Confined Impinging Jet onto a Flat Surface at $Re = 10^4$, *Aerosol Science and Technology*, **40**, 2006, 147-156.
- [4] Craft, T. J., Gragan, J. W. & Launder, B. E. (1993). Impinging jet studies for turbulence model assessment – II An examination of the performance of four turbulence models. *International Journal of Heat and Mass Transfer*, **36**, 2685-2697.
- [5] Gordon, M. & Taylor, J., Ideal copolymers and the second order transitions of synthetic rubbers. *Journal of Applied Chemistry*, **2**, 1952, 493-500.
- [6] Hennigs, C., Kockel, T. K. & Langrish, T. A. G., New measurements of the sticky behaviour of skim milk powder. *Drying Technology*, **19**, 2001, 471 – 484.
- [7] Jambunathan, K., Lai E., Moss, M.A. & Button, B.L., A review of heat transfer data for single circular jet impingement, *International Journal of Heat and Fluid Flow*, **13**, 1992, 106-115.
- [8] Konstandopolous, A. G., Particle sticking/rebound criteria at oblique impact. *Journal of Aerosol Science*, **37**, 2006, 292–305.
- [9] Murti, R. A., Paterson, A. H. J., Pearce, D. & Bronlund, J. E., The influence of particle velocity on the stickiness of milk powder. *International Dairy Journal*, **20**, 2010, 121-127.
- [10] Paterson, A. H., Bronlund, J. E. Zuo, J. Y. & Chatterjee, R., Analysis of particle-gun-derived dairy powders stickiness curves. *International Dairy Journal*, **17**, 2007, 860 – 865.
- [11] Wall, S., John, W. & Wang, H. C., Measurements of kinetic energy loss for particles impacting surfaces. *Aerosol Science and Technology*, **12**, 2007, 926 – 946.
- [12] Walmsley, M. R. W., Zhao, S., Walmsley, T. G., Neale, J. R., Atkins, M. J. & Hoffmann-Vocke, J., *Modelling Deposition of Amorphous Based Particles in an Impingement Jet*. Paper presented at the 19th International Congress of Chemical and Process Engineering, Prague, Czech Republic, 2010.
- [13] Williams, M. L., Landel, R. F. & Ferry, J. D., The temperature dependence of relaxation mechanisms in amorphous polymers and other glass-forming liquids. *Journal of the American Chemical Society*, **77**, 1955, 3701 - 3707.
- [14] Zhao, S., *Experimental and numerical investigations on skim milk powder stickiness and deposition mechanisms*. Master's of Philosophy Thesis, University of Waikato, 2009.